https://doi.org/10.3311/PPci.45300
Creative Commons Attribution

Periodica Polytechnica Civil Engineering

Experimental Study of Erosion Process under a Submerged Pipe for Unsteady Flow Conditions

Esmaeil Shaker[1,2], Seyed Mahmood Kashefipour[1], Mahmood Shafai Bejestan[1], Mohammad Bahrami Yarahmadi[1*]

[1] Department of Water Structures, Faculty of Water and Environmental Engineering, Shahid Chamran University of Ahvaz, 6135783151 Ahvaz, Iran
[2] The Head of Department of River Engineering Studies in Khuzestan Water and Power Authority (KWPA) 61335-137 Ahvaz, Iran
* Corresponding author, e-mail: m.bahrami@scu.ac.ir

Received: 26 June 2026, Accepted: 26 October 2026, Published online: 06 November 2026

Abstract

River crossing pipelines are the best and economical ways for the transit of any kind of liquids or gases from one side to another side of a river. However, under pipe erosion is a serious problem, which may finally lead to reversal and destruction of the pipeline, especially for the non-buried pipelines. Overturning and destroying the pipeline may cause the release of a significant amount of pollutants into the rivers and cause irreparable damage to the environment, aquatic and humans. Since unsteady flow conditions are generally predominant cause for scouring and sedimentation around the hydraulic structures, therefore this research was conducted to experimentally investigate the under crossing pipeline erosion for unsteady flow conditions using different hydrographs produced in a laboratory flume and clear water condition. The variables were the type of hydrograph and pipe diameter. All hydrographs were designed with the same base time, but different peak discharge and the number of peaks (duplicate hydrographs). The results showed that the depth of erosion under pipeline was significantly and directly affected by pipe diameter and the discharge of the peak of the hydrograph. Duplicate hydrographs for the same base time were found to be effective on erosion due to, the first, the rate of increasing discharge at the beginning of experiments and, the second, the cumulative shear stress- time for the first minutes of starting erosion. Six experiments were also designed to investigate the erosion for steady flow and the results were compared with the corresponding experiments for unsteady flow conditions.

Keywords

scour, river crossing pipeline, unsteady flow, hydrograph, environment

1 Introduction

Pipelines are the most common ways to transit the different types of liquids, such as oil, water, wastewater, hydrocarbons, or any type of gasses, etc., from one side to another side of rivers. Local scouring around the pipeline (especially during a flood) is an essential problem for its stability, and this process may lead to breaking in the pipeline, especially for the pipes that are laid on the river bed and without any support [1]. Also a pipeline buried in a riverbed can gradually become exposed to flow through the processes of local and general scour during flood events, even if the initial burial depth is deemed safe. High-discharge floods exacerbate bed erosion and overall bed level degradation. Finer sediments are transported downstream, leading to deposition further downstream, while coarser sediments remain upstream. This gradual process, often occurring annually, progressively reduces the pipeline's burial depth relative to the new bed surface. Additionally, the pipeline acts as a hydraulic obstacle, generating horseshoe vortices upstream and wake vortices downstream, which increase bed shear stress and excavate deeper scour holes beneath and around the pipeline. The pipeline gradually settles or becomes suspended, further amplifying shear stress. The scour hole initiates at a point and rapidly extends along the pipeline length. Factors such as high peak discharges, prolonged flood durations, mobile bed conditions (live-bed), and river morphological changes (e.g., meanders or channel shifts) intensify the depth and rate of erosion. For instance, on July 1, 2011, the 12-inch Silvertip pipeline near Laurel, Montana, ruptured at its Yellowstone River crossing, releasing approximately

Cite this article as: Shaker E., Kashefipour S. M., Shafai Bejestan, M., Bahrami Yarahmadi M. " Experimental Study of Erosion Process under a Submerged Pipe for Unsteady Flow Conditions", Periodica Polytechnica Civil Engineering, 2026. https://doi.org/10.3311/PPci.45300

1,500 barrels of crude oil into the river and floodplain, damaging fish habitats, birds, wildlife, and recreational uses [2]. Similarly, on January 17, 2015, the Poplar Pipeline owned by Bridger Pipeline Company failed upstream of Glendive, Montana, spilling about 1,200 barrels of crude oil into the Yellowstone River [3]. Also in 1994, the flooding of the San Jacinto River in Texas, USA, caused multiple pipelines to rupture, causing 34,500 barrels of crude oil and petroleum products to be discharged into the river and ignited [4]. Therefore, breaking the river crossing pipeline not only causes irreparable damage to the environment, but also causes many economic damages and is even dangerous for human health. Accordingly, given the potential hazards involved, various standards, including DNV-RP-F109 [5], emphasize lateral and vertical stability against currents. Section 3.5.3 of this standard addresses the impact of scour on pipeline embedment and the resultant reduction in soil resistance, underscoring that erosion in erodible beds can alter embedment and compromise stability. Furthermore, it recommends the use of scour models to predict such changes.

The first step for the understanding of the local scouring and/or erosion mechanism around the pipeline is recognition of the flow algorithm around it, and many scientists have published their research in this regard [6–9]. In recent years the scouring mechanism is also investigated by numerical models [10, 11]. When a pipe is installed on the river bed, the flow impact with the pipe produces some different vortices around it. At the immediate upstream of the pipe, the flow velocity becomes zero due to the impact of flow with the pipe, and the whole flow overflows from the pipe. Due to the separation phenomenon, this stagnation area makes higher hydrodynamic pressure at upstream and low pressure downstream of the pipe. The existence of a pressure gradient between both sides of the pipe, together with the flow separation phenomenon, produces a few vortices and forces at the downstream of the pipe. This hydrodynamic force washes the sediments under the pipe and, by the time, makes the eroded hole larger. The leakage flow under the pipe makes the scour depth larger, and, after a few hours, the dimensions of the hole become in equilibrium with that flow discharge [6]. Dey [9] defined the scouring process under the pipe in four consecutive steps, including scouring threshold; leakage or piping; tunnel erosion due to under pipe flow and downstream vortices; and, finally, by creating the bedform (dunes) and its migration further downstream, the dune disappears as the scour progresses. Dey [9] named this stage as Lee-wake erosion.

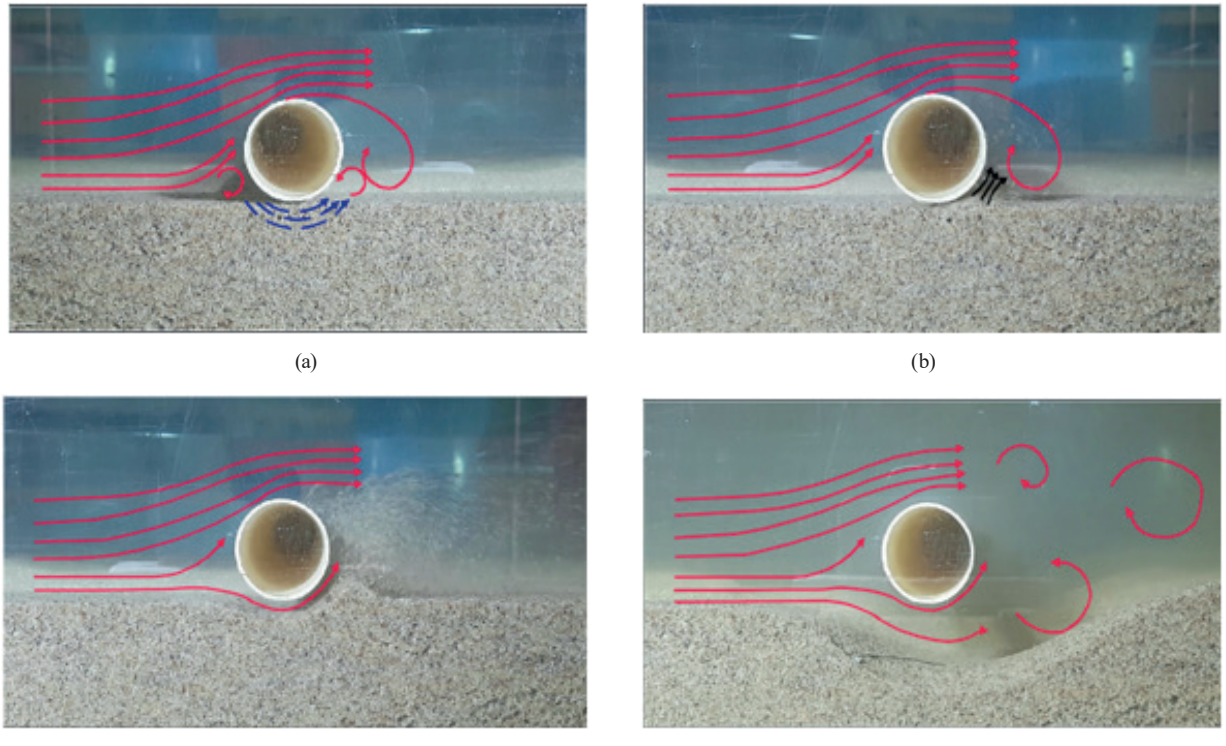


Fig. 1 Schematic figure of flow pattern and erosion under a river crossing pipeline: (a) seepage flow induction below a pipeline, (b) Piping, (c) Tunnel erosion, (d) Lee-wake erosion

These four steps are shown in Fig. 1 in which four photos were captured from a film of an experiment in the current study, and flow patterns are schematically shown on them. It is essential to clearly distinguish between the distinct physical mechanics governing these stages: the initiation of scour is primarily a pressure-driven piping process, driven by the hydrodynamic pressure differential between the upstream stagnation zone and the downstream separation zone, which forces seepage flow through the bed material. Once piping connects into a continuous slot beneath the pipe, the process transitions to shear-driven erosion (encompassing tunnel erosion and downstream lee-wake erosion), where localized flow acceleration and bed shear stress (τ) become the primary mechanisms driving bed sediment detachment and scour hole expansion.

Local erosion under the river crossing pipeline is the main cause for the collapse of the pipe, and this problem is an important subject for river engineers and environmental managers. Therefore, there are many types of research in the literature investigating this phenomenon. Dey and Singh [1] investigated the effect of many parameters on local erosion under the pipeline. The variables considered in this research were pipe diameter, pipe cross-section, the depth of approaching flow, sediment size, and sediment armoring. A part of the results extracted from this study showed an increasing value for the maximum scour depth with increasing water depth of approaching flow (the effect of this parameter for y/D more than 5 is negligible; y and D are flow depth and pipe diameter, respectively), and a decreasing value of this parameter when the armored layer formed. Azamathulla et al. [12] studied the effect of pipeline angle with the river flow path in which four angles were investigated, and they concluded that the pipeline angle had no significant effect on the maximum scour depth, and only the scour depth displaced with different angles. A numerical and experimental study was carried out by Zhao et al. [13] in which the maximum scour depth was measured for the consecutive pipelines with different pipe spacing for two different conditions, live bed (i.e., $U > U_c$; U and U_c are flow velocity and velocity for the threshold sediment movement, respectively) and clear water (i.e., $U < U_c$). The results of this research showed that the maximum scour depth for the downstream pipeline was larger than the scour depth for the upstream one. This parameter was also found to be larger for clear water conditions in comparison with the live bed since there was not wash load or fine sediment load coming from upstream for the first case. The same results were reported by Zhang et al. [14] for the same case. However, they said for the ratio of $G/D > 3$ (G = gap distance between two consecutive pipeline, D = pipe diameter), the maximum equilibrium scour depth happens under the upstream pipeline. Cui et al. [4] investigated the erosion under the crossing pipeline for different particle size riverbed sediment and steady flow condition. Their results showed that the equilibrium scour depth formed by the fine sand riverbed was the largest and about 1.5 times the pipe diameter. They also found that for the pipeline with half exposed and the clay riverbed the scour hole was very smaller than the fine sand riverbed. Li and Ma [15] investigated the scouring mechanism under the groups of submerged suspended and partially-buried river crossing pipelines for the steady flow conditions. They found that for a group of suspended parallel pipelines the ratio of G/D (gap-to-diameter ratio) is a predominant factor in scour hole size and for the partially-buried pipelines the block height and the pipeline curvature are the predominant parameters. The three-dimensional flow velocity and scouring process under the submerged parallel pipelines were numerically studied by Kolahdouzan et al. [16]. The results showed that for two parallel pipelines with a gap-distance of $0.5D$, the maximum scour hole depth was 28.6% less than the corresponding value for a single pipeline. This value was 47.6% for three parallel pipelines. Valizadeh et al. [17] investigated local scouring around buried and semi-buried pipes under different placement conditions of the pipe relative to the flow direction in a 90° mild bend. The results showed that in the condition where the pipeline passage is vertical to the flow direction, the depth of the scour hole after the pipe has the highest value.

All the above reviewed scientific research and the other several numerical and experimental published studies in the recent decades of the current literature have been carried out under steady flow conditions. The design of the river crossing submerged pipeline is generally done based on the information collected during the laboratory investigation or numerical studies for steady and long term flow conditions. However, the unsteady flow is generally predominant for scouring under pipeline in nature, and many studies show that the flow and scouring algorithm is quite different for unsteady flow in comparison with steady flow conditions [18]. In the last two decades, a new attitude has been developed for experimental and numerical studies regarding local scouring subject around different hydraulic structures in which unsteady flow conditions are usually considered [19, 20]. Based on the long term

observations, the scour hole never reaches an equilibrium stage, and its development conforms from a logarithmic trend, and this conclusion is in contrast with the studies before the year 1990. From the practical aspects, long term investigation on scour hole development is not really in nature because floods in rivers are basically time-dependent phenomena, and, in a flood hydrograph after reaching a peak value of discharge, it decreases with time [21]. Therefore, with variable discharge or velocity and as a result variable shear stress in unsteady flow, the concentration of sediment transport would be variable, and the values of transported sediments would be quite different from what usually happens for a constant discharge. The design of hydraulic structures in rivers is generally based on a maximum discharge flowing for a very long or theoretically infinite time with existing of a sediment layer with known characteristics; this time is usually called equilibrium time. In this case, the created local scouring zone is also named the equilibrium scour hole, and the process is done for equilibrium conditions. For the real terms, the flood duration is less than the equilibrium time for the scour hole development, and the discharge is variable during a flood, and it may stay at a maximum value for a short time. Therefore, the scouring of river structures after a hydrologic event is often less than what happens for equilibrium conditions [22–25].

In recent years, scientists have preferred to study and investigate scouring around the hydraulic structures under unsteady flow conditions, mostly around the bridge piers and abutments. For example, these references from current literature may be pointed out: Oliveto and Hager [21], Karimaei Tabarestani and Zarrati [24], Link et al. [25], Abolfathi et al. [26], Khajavi et al. [27], Hakim et al. [28]. Research has also been done on the effect of waves (such as sea and ocean waves) on the stability of submarine pipelines. Zhao et al. [29] numerically investigated of hydrodynamic characteristics and local scour mechanism around submarine pipelines under joint effect of solitary waves and currents. They found that when the background current was small, the solitary wave dominated the scour equilibrium state. However, when the background current was strong, the solitary wave accelerated the scour, but the background current played a leading role in the scour equilibrium state. Zhai et al. [30] studied the effect of burial depth and space between the centers of twin pipelines on the wave-seabed-twin pipelines interaction subject to waves. The results indicated that the burial depth and relative position of twin pipelines can significantly affect the wave-averaged flow velocity field and the pore-water pressure distribution as well as effective stress.

In the nature, all hydraulic structures in rivers are usually affected by different hydrographs resulting from floods and heavy raining. However, review of the literature shows that there is no comprehensive and systematic study on the scouring process under river crossing pipelines for unsteady flow conditions, in especial, for hydrographs with different peak flow, skewness and number of peaks. Therefore, in this study, the effect of the specifications of normal (Gaussian distribution) and duplicate hydrographs (two-peak and three-peak) were experimentally investigated on the maximum scour depth under the pipeline installed directly on the river bed (i.e., zero gap between pipeline and bed).

2 Materials and methods

2.1 Experimental setup

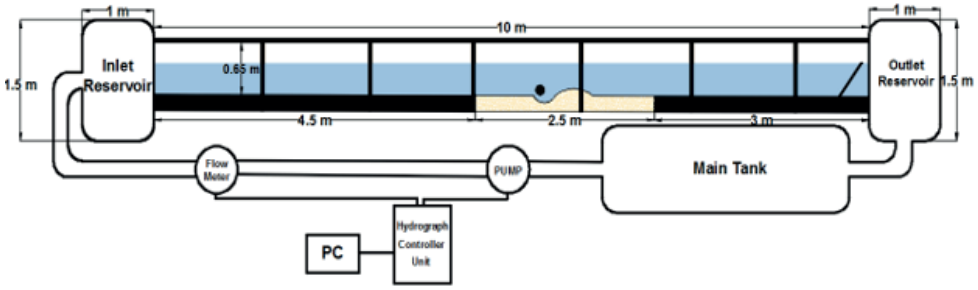
Experiments were conducted in water circulating rectangular flume with 10 m long, 0.74 m width, and 0.6 m depth in the hydraulic laboratory of Shahid Chamran University of Ahvaz, Iran. The walls and bed of this flume were made of glass and steel, respectively. At upstream and downstream of the flume, two tanks were installed, and the first one was equipped with a system to reduce water turbulence, so water flow enters into the flume calmly. All the experiments took about 2 months, and the water temperature varied between 20–21°C within this duration. The discharge was continuously measured by an electromagnetic flowmeter with an accuracy of 0.25% of the measured discharge (e.g., 40.0 ± 0.1 L/s) and was installed on the entrance pipe of the flume. Two meters of the bed in the middle of the flume was made 15 cm deeper and was filled by sand with an average diameter (d_{50}) of 0.7 mm, specific gravity of 2.65. Standard deviation of the sediment particles, i.e., $\sigma_g = \sqrt{d_{84} / d_{16}}$ was measured equal to 1.35, where d_{84} and d_{16} are diameters with 84% and 16% of particles being smaller than those, respectively. The value of standard deviation (<1.4) indicates that the sediment used was uniform [1]. Sediments were filled and leveled with the same pouring method for all experiments, so the initial conditions of sediments were the same at the start of each experiment. Pipe diameter is an important parameter affecting the amount of scour depth under the pipeline in special for the shallow rivers (Bijanvand et al., [31]). So, the pipe diameter was considered as a variable in

this research, so three pipes made from rigid Poly Vinyl Chloride (PVC) with the diameters of 20, 40, and 60 mm were used to simulate the river crossing pipeline in the experimental flume. In all experiments, the pipeline was fixed between flume's walls and installed perpendicular to the flow direction and directly on the bed. A schematic figure of the flume and its apparatus is shown in Fig. 2(a), and a general view from the flume and installed pipe can be seen in Fig. 2(b).

A system was designed to generate continuous unsteady flow, which was combined from two parts including hardware and software. The software part was uploaded and set on a computer, enabling the user to design any type of hydrographs. The hardware contained one electronic part, being matched with the software, and one inverter, which was able to control and change the pump engine speed and rotation. According to the type of hydrograph for any discharge at any time, the computer software sends a pulse to the electronic part, and it transmits this command to the inverter, and it changes the pump engine speed and, finally, discharge. The advantage of this system to manual or traditional methods is that we were able to generate completely continuous unsteady flow.

During each experiment, a camera with a quality of 12 megapixels' resolution and 60 frames per second recorded the scouring process under the pipeline, so we were able to analyze the films and pictures using a special computer-free access commercial package. The recorded films were transferred to the Free Video to JPG Converter software package and were changed to the several pictures, and the maximum scour depth was measured for any desired time using those pictures in the free Graph Grabber software package. All the scour depths were measured a few centimeters far from the wall to avoid any undesirable effect from the interaction of the wall and bed (see Bombardelli et al. [32]). To ensure measurement reliability and evaluate uncertainty, bed elevation and maximum scour depth profiles were systematically cross-checked using a digital point gage with an accuracy of ±0.1 mm installed on a precision carriage rail spanning across and along the flume. Measurements recorded via image processing were benchmarked against point gage readings across three transverse cross-sections along the pipeline length, confirming excellent agreement. Water surface elevation was similarly monitored using the digital point gage. Dey and Singh [1] also used the image processing system for the specifying time, varying maximum scour depth.

Before starting each experiment, the gate at the end of the flume was kept close, and water with a very low rate entered into the flume up to becoming full of water. The pipe was then installed at the desired point of flume perpendicular to the wall and on the bed. This pre-test part was carried out in order to prevent undesirable scouring around the pipeline.



(a)



(b)

Fig. 2 Laboratory flume and its apparatus: (a) the schematic figure, (b) a photo

2.2 Method of research

The experiments were carried out for both steady and unsteady conditions. The experimental configuration assumes a fixed pipeline without vertical movement. In natural river crossings, pipelines may settle, oscillate, or re-bury as scour progresses, introducing pipe–soil interaction feedbacks that alter local hydrodynamics and pressure fields (Sumer and Fredsøe, [8]; Cheng et al., [33]). This assumption may limit direct extrapolation of the results to field conditions and should be considered a conservative scenario. Furthermore, the experiments were conducted under clear-water scour conditions without upstream sediment supply. In real flood events, incoming bedload and suspended sediment may partially infill scour holes or reduce sediment mobility between peaks, potentially lowering scour rates compared to the present results. Given the conservative assumption of clear-water conditions, it is recommended that future studies incorporate experiments with sediment supply under live-bed conditions to achieve a more comprehensive understanding of the phenomenon. In order to make sure of clear water conditions, the maximum approach velocity (U) was kept under 95% of critical velocity (U_c) for the threshold movement of the uniform sediment. This critical velocity was calculated using the following equation proposed by Lauchlan and Melville [34]:

$$\frac{U_*}{U_{*C}} = 5.751 \log\left(5.53 \frac{y}{d_{50}}\right), \quad (1)$$

where y, d_{50} and U_{*C} are approach depth of flow, the average size of sediment, and critical shear velocity, respectively. The last parameter was calculated using the Shields diagram and the other two parameters. In primary experiments, it was observed that the threshold of sediment movement happened for the discharge of 35 L/s or its corresponding Froude number value of 0.27. In order to specify the base flow discharge of hydrograph, the worst conditions for scouring (i.e., pipe with 60 mm diameter) was considered, and, it was found that with a discharge of 15 L/s or its corresponding Froude number value of 0.11, there was not any erosion under the pipeline. So, the base flow discharges of all hydrographs were considered 15 L/s, and the maximum peak discharges of hydrographs were set as 33 L/s to make sure of the clear water conditions.

At the upstream of the pipeline, the depth velocity distribution must be uniform, so the distance of pipe installation from the upstream end of the flume should be far enough for having developed approach flow and uniform velocity distribution. To find the best place of pipeline installation, velocities through the depth and for six cross-sections with 0.5 m, 1.0 m, 1.5 m, 2.0 m, 2.5 m, and 3.0 m from the pipeline towards upstream were measured using a 3D electromagnetic velocity meter with a constant discharge of 30 L/s and depth of 18 cm. Fig. 3 illustrates the depth velocity distribution for those cross-sections; as it is seen from this figure, the velocity profiles were relatively uniform along the flume and were almost in logarithmic form, showing the developed flow boundary layer [35]. In this figure, the x-axis refers to the longitudinal velocity at any depth (y in the y-axis).

In nature, meteorological and physiographic parameters affect the form of hydrographs. For example, intensity and duration of precipitation, evaporation, transpiration, basin form and dimensions, average slope, soil properties, land use, green cover, etc. are some of the effective parameters [36]. The rising limb is usually affected by meteorological parameters, whereas the recession limb of the hydrograph is influenced by physiographic parameters [37]. So, it may be possible to have duplicate hydrographs with different peaks. There are many reported examples of duplicate hydrographs in the literature, with two or more peaks during one event [38]. Therefore, in this study, a number of 21 experiments were designed and run, in which 6 of them were for steady conditions, 3 for normal or Gaussian distribution hydrographs with one-peak, and 12 of them were for duplicate hydrographs. A summary of the implemented experiments is illustrated in Table 1.

This study mainly focuses on the effect of unsteady flow on local scour under a submerged pipeline and compares with steady flow conditions. Also the effect of rising and recession limbs of hydrographs on time progress of scour depth are investigated. Therefore, the total running time for all hydrographs was chosen as 120 min, as well as the duration of experiments for steady conditions. The experiments for the steady conditions were designed based on the

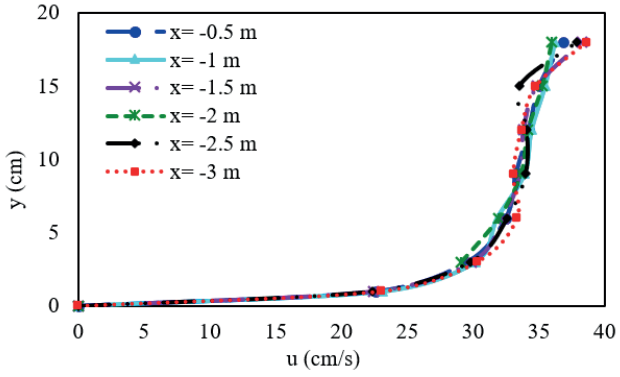


Fig. 3 Depth velocity distribution for some cross-sections of the flume

Table 1 Specification of experiments for steady and unsteady flows

Test No.	Type	Test Name	D_p (mm)	t_{p1} (min)	t_{p2} (min)	t_{p3} (min)	Q_s (L/s)	Q_{p1} (L/s)	Q_{p2} (L/s)	Q_{p3} (L/s)	Freqn*
1	Steady	S1	20	-	-	-	33	-	-	-	-
2	Steady	S2	40	-		-	33	-	-	-	-
3	Steady	S3	60	-	-	-	33	-	-	-	-
4	Steady	S4	20	-	-	-	27	-	-	-	-
5	Steady	S5	40	-	-	-	27	-	-	-	-
6	Steady	S6	60	-	-	-	27	-	-	-	-
7	Unsteady	U1	20	60	-	-	-	33	-	-	1
8	Unsteady	U2	40	60	-	-	-	33	-	-	1
9	Unsteady	U3	60	60	-	-	-	33	-	-	1
10	Unsteady	U4	20	30	90	-	-	33	33	-	2
11	Unsteady	U5	40	30	90	-	-	33	33	-	2
12	Unsteady	U6	60	30	90	-	-	33	33	-	2
13	Unsteady	U7	20	20	60	100	-	33	33	33	3
14	Unsteady	U8	40	20	60	100	-	33	33	33	3
15	Unsteady	U9	60	20	60	100	-	33	33	33	3
16	Unsteady	U10	20	30	90	-	-	33	27	-	2
17	Unsteady	U11	40	30	90	-	-	33	27	-	2
18	Unsteady	U12	60	30	90	-	-	33	27	-	2
19	Unsteady	U13	20	30	90	-	-	27	33	-	2
20	Unsteady	U14	40	30	90	-	-	27	33	-	2
21	Unsteady	U15	60	30	90	-	-	27	33	-	2

*One Peak: Freq1, Two Peak: Freq2, Three Peak: Freq3

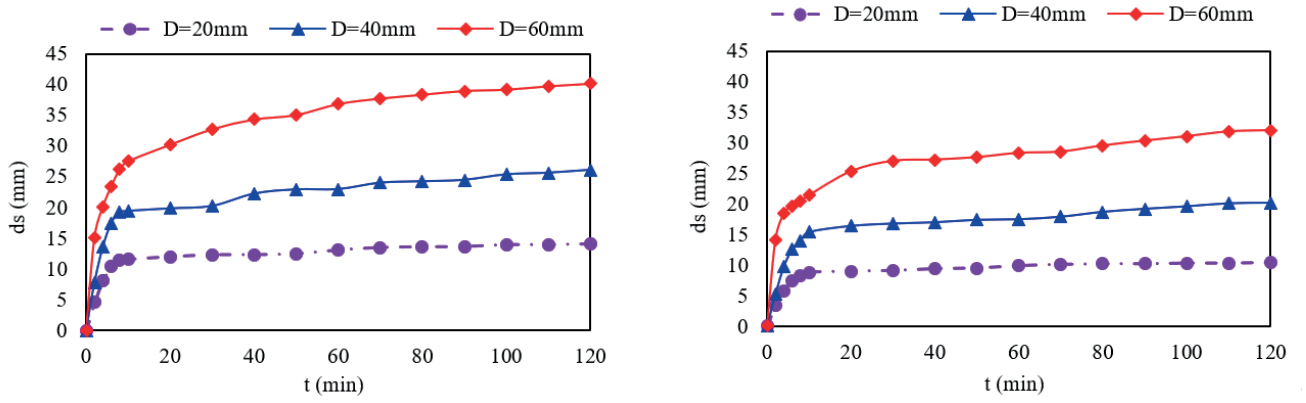


Fig. 4 Time-varying of the maximum scour depth for steady conditions and discharge of (a) 33 L/s, (b) 27 L/s

peak flow of the hydrographs (i.e., 33 and 27 L/s) and three pipe diameters. Three types of hydrographs were defined as normal with one peak (Freq1), two peaks (Freq2), and three peaks (Freq3) with the same amount of the peak discharge and total base time. Two hydrographs were also defined with two different peaks, and a total of 15 hydrographs were produced (see Table 1). In this table, t_{p1}, t_{p2}, and t_{p3} refer to the time of peak discharge of hydrographs for the first, second, and third peaks, respectively. Q_s is the constant discharge for steady flow experiments, and Q_{p1}, Q_{p2}, and Q_{p3} are the peak discharges for the first, second, and third peaks of hydrographs, respectively.

3 Results and discussion

3.1 Steady conditions experiments

The experimental observations showed that after starting each experiment, leakage under the pipe started due to the existing pressure gradient at the upstream and

downstream of the pipe. Piping was the second stage of the scouring under the pipe, and, with an increase in leakage velocity, a large amount of sediment was washed under the pipe due to higher shear stress, and the tunnel erosion was formed, and, finally, the dune bedform was created and moved downstream. As observed, the transition from pressure-driven seepage (piping initiation) to velocity- and shear-stress-driven erosion (tunnel and lee-wake erosion) marks the primary physical boundary in scour evolution. Jensen et al. [39] reported the same process for steady conditions (see Fig. 1). After tunnel erosion and when the created slot under the pipeline became large enough and due to having two flows from above and beneath the pipeline, a few vortices were created downstream of the pipe. These vortices caused the continuing of scouring under the pipeline up to reaching an equilibrium stage.

Figs. 4(a, b) show the time-varying of the maximum scour depth (d_s) with the constant discharges of 33 and 27 L/s or the corresponding Froude numbers of 0.25 and 0.2, respectively. In these figures, the measured maximum scour depths were for the pipe diameters of 20, 40, and 60 mm. The parameter d_s was measured under the pipeline for any time by analyzing the pictures extracted from the recorded films. It should be noticed that the total time for each experiment with steady conditions was set to 120 min, which was equal to the base flow time of hydrographs. It seemed that, in this time, the maximum scour depth had not reached its equilibrium condition; however, this stage was not important because the comparison of steady and unsteady conditions for the scouring process was a part of the aims in this study.

Figs. 4(a, b) also show the interactive effects of pipe diameter and discharge on maximum scour depth for steady conditions. As could be seen from these figures, the maximum scour depth significantly increased with increasing pipe diameter; for example, the final scour depth for the pipe with 60 mm diameter was measured 1.85 times of what was measured for the pipe with 20 mm diameter (for the discharge of 33 L/s). This difference could be due to the higher pressure gradient and higher velocity under the pipeline for the first one in comparison with the second one. Increasing discharge with the same depth produced higher velocity and shear stress, so the maximum scour depths for maximum discharge (i.e., 33 L/s) were higher than the corresponding values for lower discharge (i.e., 27 L/s). The important point was that more than 70% of the final scour depth occurred in the first few minutes of starting experiments (see Table 2). This table illustrates the percentages of the maximum scour depth at any time in comparison with the total considered time during the scouring process. It should be explained that with increasing the scour depth under pipeline the velocity and shear stress of water flowing under the pipe decrease and as a result the rate of developing the scour hole dimensions decreases and at the equilibrium stage for a desired discharge this development will completely stop. The time series measured depths of the scour hole clearly show this finding (Table 2). This phenomenon was also observed for the unsteady flow conditions, as described in following sections.

3.2 Unsteady flow conditions

3.2.1 The effect of hydrograph with normal distribution on scouring

River flow during floods is in unsteady conditions, so experimental investigations of the scouring around different hydraulic structures under unsteady conditions are more realistic. The flow algorithms for steady and unsteady conditions were the same, but the amount of bed shear stress for unsteady conditions was variable according to the type and form of hydrographs. Since the clear water conditions were assumed for the proposed hydrographs for any amount of flow, and the peak of each hydrograph was chosen as the flow rate for the experiments with steady conditions, so the scouring under pipelines for unsteady conditions was expected to be less than their corresponding values for steady conditions. Figs. 5(a–c) illustrate the time-varying maximum scour depth for steady (Q = 33 L/s) and unsteady flow conditions, i.e. hydrograph with normal distribution and T_p = 60 min, Q_p = 33 L/s, where T_p and Q_p are the time and discharge of the peak point, respectively, for three pipe diameters of 20, 40, 60 mm, respectively. The hydrograph is also shown in these figures using the second axis. The time-varying amount of the maximum scour depth for steady and unsteady conditions are compared in Table 3. This table shows the ratio of the maximum scour depth for unsteady to steady conditions in the form of a percentage.

Table 2 Percentage of the maximum scour depth at any time for different discharges and pipe diameters

Time (min)	Q_s = 27 L/s			Q_s = 33 L/s		
	D_p = 20 mm	D_p = 40 mm	D_p = 60 mm	D_p = 20 mm	D_p = 40 mm	D_p = 60 mm
10	83	76	66	82	74	68
20	87	80	79	85	76	75
40	90	85	84	88	85	85
80	98	92	92	97	94	94
120	100	100	100	100	100	100

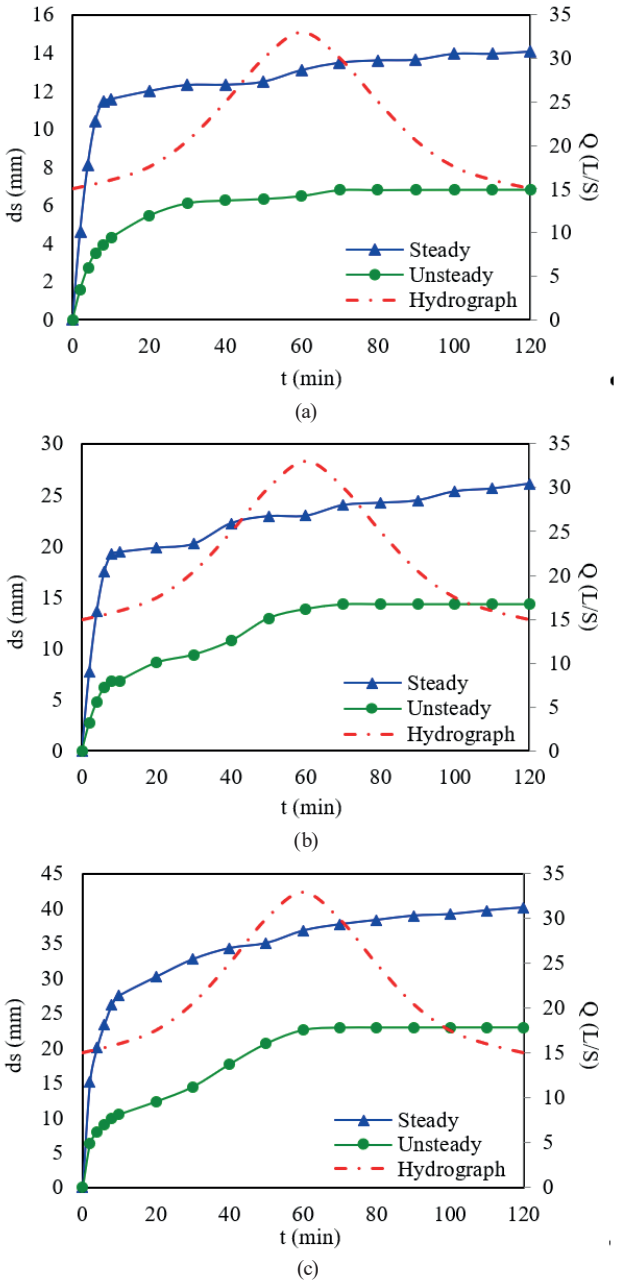


Fig. 5 Time-varying of the maximum scour depth for steady and unsteady conditions, and the hydrograph with normal distribution for pipes with a diameter of (a) 20 mm, (b) 40 mm, (c) 60 mm

Table 3 The ratio of the maximum scour depth for unsteady (hydrograph with normal distribution) to steady (Q = 33 L/s) conditions (%)

Time (min)	Pipe Diameter (mm)		
	20	40	60
10	37	35	38
20	45	44	41
40	51	48	52
80	50	59	60
120	48	55	58

As could be seen from Fig. 5, the slope of the scouring depth-time curve for steady flow conditions for all pipe diameters was steeper than the corresponding values for unsteady conditions. This was due to the inserting of the maximum bed shear stress from the beginning of the experiment for steady flow conditions, which caused more scouring at the starting time. Whereas, during each hydrograph, the bed shear stress at the starting time was very low and gradually increased up to a maximum value of bed shear stress.

The scouring depth-time curve for unsteady conditions after reaching the peak flow of hydrograph did not change since, along the recession limb of hydrograph, bed shear stress dramatically decreased. Oliveto and Hager [21] reported the same results for the scouring depth around bridge pier and abutment. Chang et al. [40] concluded that the scour depth around the bridge pier increased with increasing discharge along the rising limb of hydrograph up to its peak. Also, they said that the recession or falling limb of hydrograph had no significant effect on scouring depth. Karimaei Tabarestani and Zarrati [24] verified their experimental scouring depth results around bridge pier with Stepped Hydrograph Model and analyzed the effect of base time of hydrograph, as well as the rising and recession limbs, on scouring depth in high range time, i.e., 1 min to 237 min.

The pipe diameter had the same effect on the maximum scour depth for steady and unsteady conditions. So, with increasing pipe diameter from 20 mm to 60 mm, the maximum scour depth increased about 240% (see Fig. 5).

3.2.2 The effect of duplicate hydrographs with the same peaks on scouring

Hydrological and physiographic characteristics of the drainage basin, such as concentration and traveling time, drainage intensity, duration and intensity of precipitation event, etc., make different types and forms of hydrographs. For example, a hydrograph produced from an event, which was happened from 21 March to 30 April 2019 in the southwest of Iran, Karkheh Basin, is shown in Fig. 6, which is a duplicate hydrograph with two different peaks. Thus, in this part, the effect of duplicate hydrographs with the same peaks on scouring under pipeline was experimentally investigated. For this purpose, the normal hydrograph (Freq1) was converted to a two-peak hydrograph with t_{p1} = 30 min and t_{p2} = 90 min (Freq2) and three-peak hydrograph with t_{p1} = 20 min, t_{p2} = 60 min, and t_{p3} = 100 min (Freq3). For these hydrographs, the peak

value was 33 L/s (see Table 1), and are shown in Fig. 7(a). Two different hydrographs were also produced with two-peaks, but different in peak discharge values, i.e., 27 and 33 L/s, and are illustrated in Fig. 7(b).

Figs. 8(a–c) show the time-varying of the maximum scour depth under the pipeline (d_s) for three hydrographs, i.e., normal (Freq1), two-peak (Freq2), and three-peak (Freq3) hydrographs, for three pipe diameters of 20, 40, and 60 mm, respectively. The maximum scour depth for Freq2 was higher than Freq1 for the whole experiment time, but, for Freq3, the depth-time curve for scouring

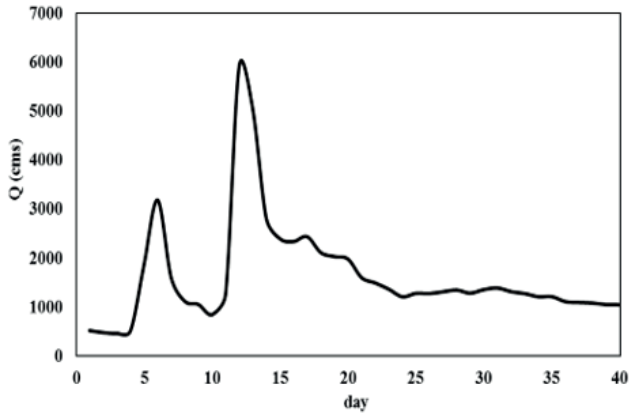


Fig. 6 The time-discharge curve in the form of the duplicate hydrograph (Karkheh Basin-Iran, Spring 2019)

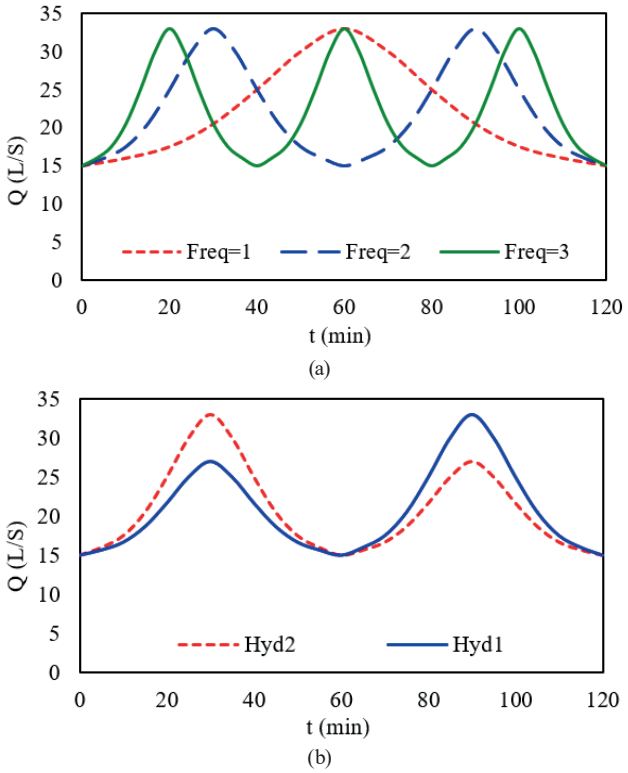


Fig. 7 Typical hydrograph (a) normal, two-peak, and three-peak, (b) two-peak with different discharge values

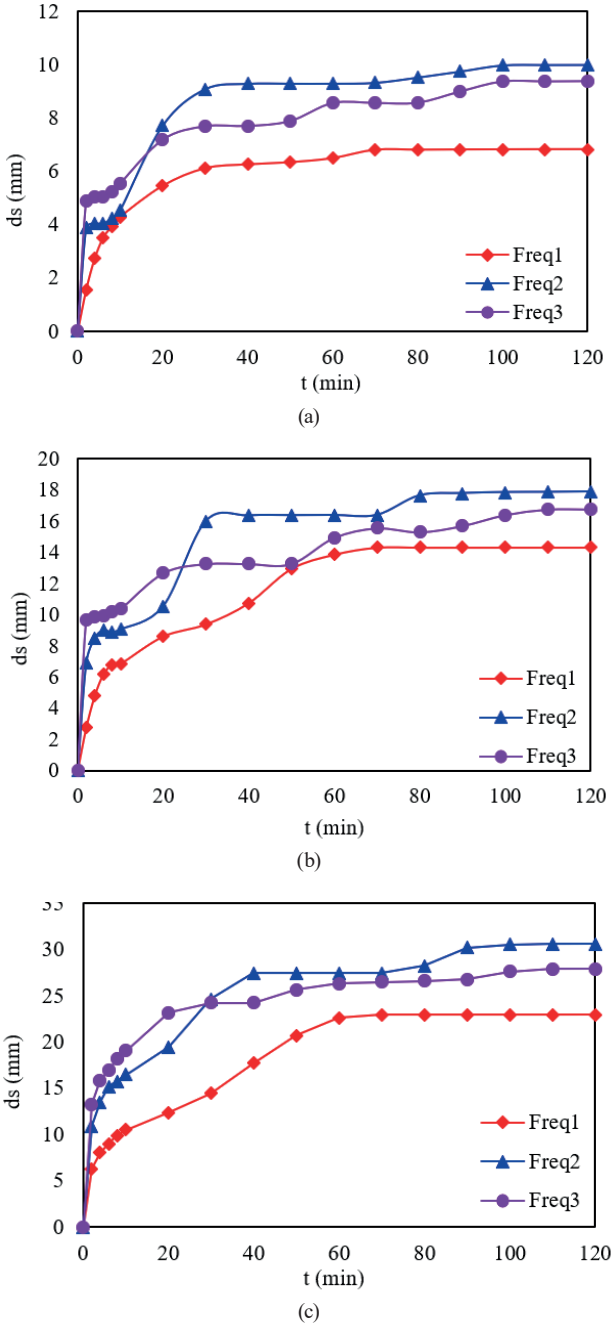


Fig. 8 Time-varying of the maximum scour depth under pipeline with a diameter of (a) 20 mm, (b) 40 mm, (c) 60 mm

at the beginning time was higher, and then it came under the depth-time curve for Freq2 (see Fig. 8). One thinks that the final maximum scour depth should be higher for Freq3 than Freq2 due to three peaks and, as a result, three high shear stresses. But as seen in Fig. 8, the results were contrary to our expectations. The reason for this behavior of scouring under the pipelines could be explained using the time-varying of the important unsteady characteristic of hydrographs, i.e., bed shear stress (τ). This parameter is variable during the flood hydrograph and is

calculated using shear velocity (u_*), which is defined as $u_* = \sqrt{\tau / \rho} = \sqrt{gRS_e}$, where ρ, g, and R are water density, acceleration due to gravity, and hydraulic radius, respectively. S_e is the slope of the energy line and can be calculated using the Manning or Chezy equations [41]. Shear stress is a key parameter for scour holes development and equilibrium, and its accurate estimation is so important; Palermo et al. [42] developed a theoretical method for shear-stress estimation at 2D equilibrium scour holes.

Fig. 9 illustrates the calculated time-varying bed shear stress for those aforementioned three types of hydrographs, i.e., Freq1, Freq2, and Freq3. The main cause for erosion and movement of sediments was this important parameter, i.e., bed shear stress. As it is clear from Fig. 9, this parameter had a rank of Freq3 > Freq2 > Freq1 for the first 20 min of starting experiments. Thus, d_s at the beginning of the experiments had the same rank as above for considered duplicate hydrographs. Furthermore, the gradient of increasing discharge for Freq1 up to the first peak was 0.55 L/s per min; this value for Freq2 and Freq3 became 1.1 and 1.65 L/s per min, i.e., two and three times of the first one, respectively.

As could be seen, by the time, the curve depth-time of Freq3 came under the curve of Freq2 (see Fig. 8). Two points should be considered here; first, the enclosed area between the curve and x-axis is defined as bed shear stress-time ($\tau - t$) parameter and expresses the amount of inserted momentum along the bed per unit area by flood hydrograph. Second, many scientists reported that more than 80% of the final scour depth (equilibrium stage) around hydraulic structures happens within the first 20%–30% of the time after the start of the experiment [43–44]. The results in this study confirmed this statement for under pipeline scouring (see Table 2), with this time value being about 40 min for the experiments in this study. The bed shear stress-time parameter ($\tau - t$) was calculated for this

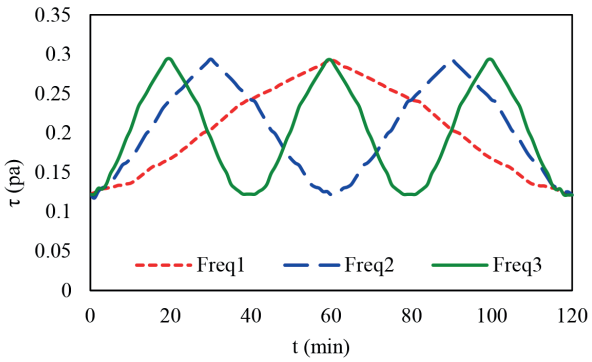


Fig. 9 Time-varying of bed shear stress for hydrographs Freq1, Freq2, and Freq3

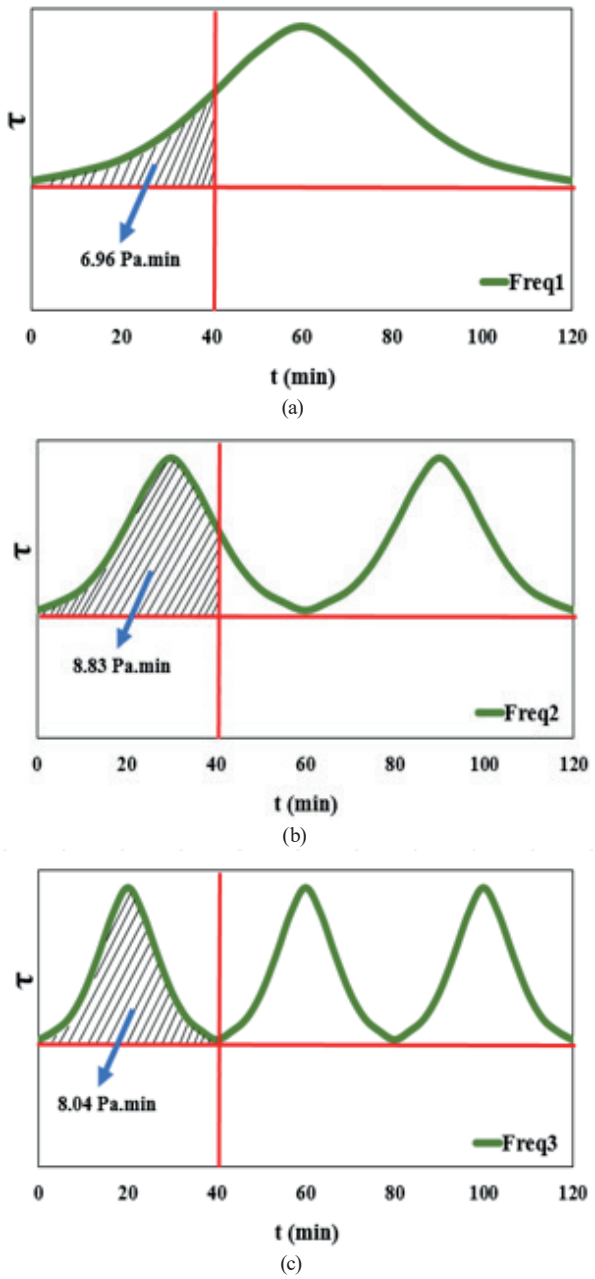


Fig. 10 Schematic figure of bed shear stress-time variation for three different hydrographs (a) normal, (b) two-peak, (c) three-peak

period and for three curves in Fig. 9 and are schematically shown in Fig. 10 (shaded area), with the rank of these values being as Freq2 > Freq3 > Freq1. These values were calculated as 8.83, 8.04, and 6.96 Pa-min for the hydrographs Freq2, Freq3, and Freq1, respectively. For the local scouring process around hydraulic structures, the first 20%–30% of starting time is very important, and after that, the potential for scouring significantly decreases [43–44].

Therefore, this discussion confirmed that why scouring at the beginning of the experiment for Freq3 was higher, but the amount of the final maximum scour depth under

Table 4 Comparison of the increase of the maximum scour depth at the end of each small hydrograph related to pre-hydrograph in a duplicate hydrograph for different pipe diameters

Pipe Diameter (mm)	Hydrograph	Second Hydrograph to the First One (%)	Third Hydrograph to the Second One (%)
20	Freq2	8	-
	Freq3	12	8
40	Freq2	9	-
	Freq3	15	9
60	Freq2	11	-
	Freq3	9	4

the pipeline was higher for the two-peak (Freq2) than three-peak (Freq3) hydrographs.

Freq1 had one single hydrograph (base time 0–120 min), Freq2 had two hydrographs (base time 0–60–120 min), and Freq3 had three hydrographs (base time 0–40–80–120 min), as shown in Fig. 7(a). The maximum scour depth was measured using the recorded films after passing each hydrograph (i.e., at the time 60 min and 120 min for Freq2 and at 40 min, 60 min, and 120 min for Freq3), so we were able to compare the amount of scouring after each small hydrograph in a duplicate hydrograph. Table 4 shows the increase in the percentage of the maximum scour depth after each hydrograph was compared to the pre-hydrograph.

3.2.3 The effect of duplicate hydrographs with different peaks on scouring

One of the very common types of duplicate hydrographs in rivers for the flood events are duplicate hydrograph with two consecutive different peaks (see Fig. 7(b)). In this section, the effect of these types of hydrographs on scouring depth under pipeline has been investigated (see Table 1, Experiments 16–21). Two forms were considered here, 1- the first peak was equal 27 L/s, and the second one was 33 L/s (Hyd1 or D1 in Fig. 7(b)), 2- the first peak was 33 L/s, and the second one was 27 L/s (Hyd2 or D2 in Fig. 7(b)). These hydrographs, as well as the time-varying of the maximum scour depth under the pipeline, are shown in Figs. 11(a–c) for the pipe diameters of 20, 40, and 60 mm, respectively. As could be seen from these figures, although the total bed shear stress values for both hydrographs were the same, the time development of the maximum scour depths under the pipeline, as well as the final maximum scour depths created by Hyd1, was less than the corresponding values generated by passing the Hyd2 hydrograph. As it was explained for similar shape of hydrographs in the previous section, two reasons could

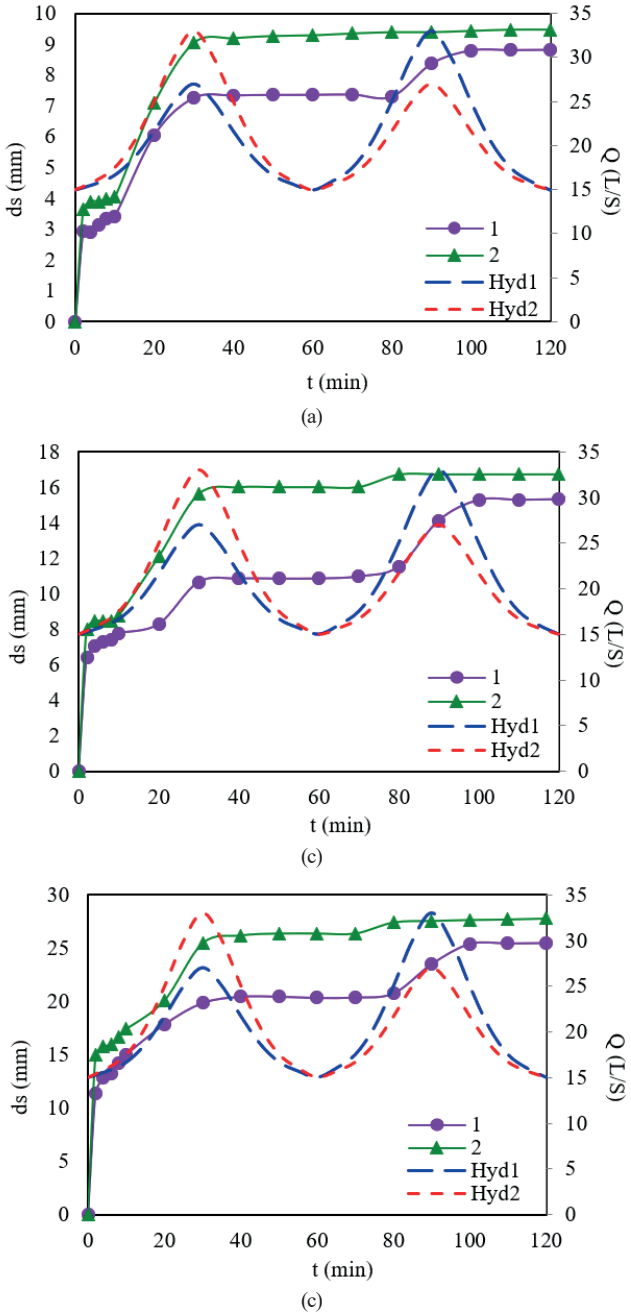


Fig. 11 Time-varying of the maximum scour depth under pipeline for Hyd1 and Hyd2 and for pipe diameters (a) 20 mm, (b) 40 mm, (c) 60 mm

be pointed out for this phenomenon; 1) the gradient of increasing discharge at the beginning of experiment was higher for Hyd2 than Hyd1 hydrographs, 2) the stress-time parameter, which showed the amount of inserted momentum along the bed per unit area at the beginning of experiment, was also higher for Hyd2 than Hyd1.

An important and notable point is how repeatable the measurements made in this study are and how likely they are to occur in practice or under similar conditions. This certainly requires further testing, taking into account other

conditions. While individual measurement accuracy was verified across three cross-sections using a digital point gage, full systematic experimental repetitions were not conducted across all 21 hydrograph tests due to operational and time constraints. This lack of complete experimental repetition is acknowledged as a limitation of the present study. Future research should include systematic repeated runs to formally quantify experimental repeatability across different hydrograph shapes and flow conditions.

4 Conclusions

The main aim of this study was to experimentally investigate the effect of the unsteadiness flow characteristics on the scouring process under the river crossing submerged pipeline. For this reason, the maximum scour depth under pipeline for steady and unsteady flow conditions (hydrographs with different hydrological characteristics) were measured and analyzed. The hydrographs were produced using a new and well-designed instrument, which was a combination of hardware and software, enabling the users to create any type of continuous hydrograph. According to the results in this study, the following conclusions can be summarized:

1. The maximum scour depth was increased with increasing pipe diameter for both steady and unsteady conditions. For example, the scouring depth was increased by 85% for a pipe diameter of 60 mm in comparison with its value for 20 mm under steady conditions.
2. A large amount of scouring under the pipeline for steady conditions happened in the first few minutes of each experiment, so, in this study, for the different pipe diameters considered, a value of 68% to 82% final scouring depth occurred for the first 10 min or about 8% of the total considered time. Whereas for unsteady conditions, the final scouring depth happened for the peak of the hydrograph, and after that, it remained constant. So, the final maximum scour depths for unsteady conditions were generally less than the corresponding values for steady conditions, with the ratio of these values being 35% to 60% (unsteady to steady) for the considered pipe diameters. This was because, in a hydrograph, the amounts of discharges varied from a small base flow to a maximum value (peak), and, therefore, the inserted bed shear stresses by hydrograph were different from a small value to a maximum one.
3. Another important conclusion from this research was that the gradient of increasing discharge for the rising limb of hydrograph was a dominant parameter in scouring under the pipeline.
4. The form of duplicate hydrographs was an important parameter, affecting the final scouring under the pipeline. For example, the measured scour depth for the duplicate hydrograph with two different peaks (the higher one first) was greater than the other hydrograph with the lower peak value first. This was due to the rate of increasing discharge, as well as the amount of shear stress at the beginning of experiments.

Acknowledgments

The authors are grateful to the Research Council of Shahid Chamran University of Ahvaz for financial support (SCU. WH99.31373).

References

[1] Dey, S., Singh, N. "Clear-water scour below underwater pipelines under steady flow", Journal of Hydraulic Engineering, 134(5), pp. 588–600, 2008. https://doi.org/10.1061/(ASCE)0733-9429(2008)134:5(588)

[2] USEPA "Silvertip Pipeline Incident Response Report", United States Environmental Protection Agency, Region 8, Helena, MT, USA, 2011.

[3] NTSB "Pipeline Accident Brief: Hazardous Liquid Pipeline Failure, Yellowstone River Crossing", National Transportation Safety Board, Washington, D.C., USA, 2015.

[4] Cui, F., Du, Y., Hao, X., Peng, S., Bao, Z., Peng, S. "Experimental study on local scour and related mechanical effects at river-crossing underwater oil and gas pipelines", Advances in Civil Engineering, 2021, 6689212, 2021. https://doi.org/10.1155/2021/6689212

[5] DNV "DNV-RP-F109: On-bottom stability design of submarine pipelines", Det Norske Veritas (DNV), Høvik, Norway, 2021.

[6] Mao, Y. "The Interaction Between a Pipeline and an Erodible Bed", Technical University of Denmark, Lyngby, Denmark, 1988.

[7] Chiew, Y. M. "Mechanics of local scour around submarine pipelines", Journal of Hydraulic Engineering, 116(4), pp. 515–529, 1990. https://doi.org/10.1061/(ASCE)0733-9429(1990)116:4(515)

[8] Sumer, B. M., Fredsøe, J. "The Mechanics of Scour in the Marine Environment", In: Advanced Series on Ocean Engineering: Vol. 17, World Scientific Utopia Press Pte. Ltd, Singapore, 2002. https://doi.org/10.1142/4942

[9] Dey, S. "Fluvial Hydrodynamics", Springer Publication, New York, NY, USA, 2014.

[10] Fuhrman, D. R., Baykal, C., Sumer, B. M., Jacobsen, N. G., Fredsøe, J. "Numerical simulation of wave-induced scour and backfilling processes beneath submarine pipelines", Coastal Engineering, 94, pp. 10–22, 2014. https://doi.org/10.1016/j.coastaleng.2014.08.009

[11] Ahmad, N., Bihs, H., Myrhaug, D., Kamath, A., Arntsen, Ø. A. "Numerical modelling of pipeline scour under the combined action of waves and current with free-surface capturing", Coastal Engineering, 148, pp. 19–35, 2019. https://doi.org/10.1016/j.coastaleng.2019.02.008

[12] Azamathulla, H. M., Yusoff, M. A. M., Hasan, Z. A. "Scour below submerged skewed pipeline", Journal of Hydrology, 509(13), pp. 615–620, 2014. https://doi.org/10.1016/j.jhydrol.2013.11.058

[13] Zhao, M., Vaidya, S., Zhang, Q., Cheng, L. "Local scour around two pipelines in tandem in steady current", Coastal Engineering, 98, pp. 1–15, 2015. https://doi.org/10.1016/j.coastaleng.2015.01.001

[14] Zhang, Q., Draper, S., Cheng, L., Zhao, M., An, H. "Experimental study of local scour beneath two tandem pipelines in steady current", Coastal Engineering Journal, 59(1), 1750002-1-1750002-22, 2017. https://doi.org/10.1142/S0578563417500024

[15] Li, B., Ma, H. "Scouring mechanism of suspended and partially-buried pipelines under steady flow", Coastal Engineering, 177, 104201, 2022. https://doi.org/10.1016/j.coastaleng.2022.104201

[16] Kolahdouzan, F., Afzalimehr, H., Siadatmousavi, S. M., Jourabloo, A., Ahmad, S. "The effect of pipeline arrangement on velocity field and scouring process", Water, 15(7), 1321, 2023. https://doi.org/10.3390/w15071321

[17] Valizadeh, R., Arman, A., Ghobadian, R. "The effect of the pipe angle and protective inclined apron on the scouring and sedimentation pattern around a semi-buried pipe in a 90º bend", Ocean Engineering, 286(2), 115711, 2023. https://doi.org/10.1016/j.oceaneng.2023.115711

[18] Lu, J., Shi, Z. Z., Hong, J. H., Lee, J. J., Raikar, R. "Temporal variation of scour depth at nonuniform cylindrical piers", Journal of Hydraulic Engineering, 137(1), pp. 45–56, 2011. https://doi.org/10.1061/(ASCE)HY.1943-7900.0000272

[19] Oliveto, G., Hager, W. H. "Temporal evolution of clear-water pier and abutment scour", Journal of Hydraulic Engineering, 128(9), pp. 811–820, 2002. https://doi.org/10.1061/(ASCE)0733-9429(2002)128:9(811)

[20] Palermo, M., Pagliara, S. "Effect of unsteady flow conditions on scour features at low-head hydraulic structures", Journal of Hydro-environment Research, 19, pp. 168–178, 2018. https://doi.org/10.1016/j.jher.2017.04.001

[21] Oliveto, G., Hager, W. H. "Further results to time-dependent local scour at bridge elements", Journal of Hydraulic Engineering, 131(2), pp. 97–105, 2005. https://doi.org/10.1061/(ASCE)0733-9429(2005)131:2(97)

[22] Su, C. C., Lu, J. Y. "Measurements and prediction of typhoon-induced short-term general scours in intermittent rivers", Natural Hazards, 66, pp. 671–687, 2013. https://doi.org/10.1007/s11069-012-0509-6

[23] López, G., Teixeira, L., Ortega-Sánchez, M., Simarro, G. "Estimating final scour depth under clear-water flood waves", Journal of Hydraulic Engineering, 140(3), pp. 725–742, 2014. https://doi.org/10.1061/(ASCE)HY.1943-7900.0000804

[24] Karimaei Tabarestani, M., Zarrati, A. R. "Local scour calculation around bridge pier during flood event", KSCE Journal of Civil Engineering, 21, pp. 1462–1472, 2017. https://doi.org/10.1007/s12205-016-0986-3

[25] Link, O., Castillo, C., Pizarro, A., Rojas, A., Ettmer, B., Escauriaza, C., Manfreda, S. "A model of bridge pier scour during flood waves", Journal of Hydraulic Research, 55(3), pp. 310–323, 2017. https://doi.org/10.1080/00221686.2016.1252802

[26] Abolfathi, S., Kashefipour, S. M., Fuhrman, D. R., Shafaei Bajestan, M. "Temporal scouring and backfilling processes around a pile group subject to unsteady hydrographs", Ain Shams Engineering Journal, 13(2), 101565, 2022. https://doi.org/10.1016/j.asej.2021.08.008

[27] Khajavi, M., Kashefipour, S. M., Shafai Bejestan, M. "Bridge abutment protection against scouring for unsteady flow conditions", Periodica Polytechnica Civil Engineering, 66(1), pp. 310–322, 2022. https://doi.org/10.3311/PPci.18892

[28] Hakim, M., Bahrami Yarahmadi, M., Kashefipour, S. M. "Use of spur dikes with different permeability levels for protecting bridge abutment against local scour under unsteady flow conditions", Canadian Journal of Civil Engineering, 49(12), pp. 1842–1854, 2022. https://doi.org/10.1139/cjce-2021-0476

[29] Zhao, E., Dong, Y., Tang, Y., Sun, J. "Numerical investigation of hydrodynamic characteristics and local scour mechanism around submarine pipelines under joint effect of solitary waves and currents", Ocean Engineering, 222, 108553, 2021. https://doi.org/10.1016/j.oceaneng.2020.108553

[30] Zhai, Y., Zhang, J., Guo, Y., Tang, Z., Zhang, T. "Study of wave-induced seabed response around twin pipelines in sandy seabed through laboratory experiments and numerical simulations", Ocean Engineering, 244, 110344, 2022. https://doi.org/10.1016/j.oceaneng.2021.110344

[31] Bijanvand, S., Kashefipour, S. M., Yarahmad, M. B. "Experimental Investigation on Specifications of Scouring Hole Under the Pipelines Across the Waterway Under Steady Flow", Journal of Irrigation Sciences and Engineering, 43(3), pp. 117–131, 2021. https://doi.org/10.22055/jise.2021.36184.1937

[32] Bombardelli, F. A., Palermo, M., Pagliara, S. "Temporal evolution of jet induced scour depth in cohesiveness granular beds and the phenomenological theory of turbulence", Physics of Fluids, 30(8), 085109, 2018. https://doi.org/10.1063/1.5041800

[33] Cheng, L., Yeow, K., Zang, Z., Li, F. "3D scour below pipelines under waves and combined waves and currents", Coastal Engineering, 83, 137–149, 2014. https://doi.org/10.1016/J.coastaleng.2013.10.006

[34] Lauchlan, C. S., Melville, B. W. "Riprap protection at bridge piers", Journal of Hydraulic Engineering, 127(5), pp. 412–418, 2001. https://doi.org/10.1061/(ASCE)0733-9429(2001)127:5(412)

[35] Chow, V. T. "Open Channel Hydraulics", McGraw-Hill, New York, NY, USA, 1959.

[36] Hannah, D., Smith, B., Gurnell, A., Mcgregor, G. "An approach to hydrograph classification", Hydrological Processes, 14(2), pp. 317–338, 2000. https://doi.org/10.1002/(SICI)1099-1085(20000215)14:2<317::AID-HYP929>3.0.CO;2-T

[37] Chow, V. T., Maidment, D. R., Mays, L. W. "Applied Hydrology", McGraw-Hill, New York, NY, USA, 1988.

[38] Váňová, V., Langhammer, J. "Modelling the impact of land cover changes on flood mitigation in the upper Lužnice basin", Journal of Hydrology and Hydromechanics, 59(4), pp. 262–274, 2011. https://doi.org/10.2478/v10098-011-0022-8

[39] Jensen, B. L., Sumer, B. M., Jensen, H. R., Fredsoe, J. "Flow around and forces on a pipeline near a scoured bed in steady current", Journal of Offshore Mechanics and Arctic Engineering, 112(3), pp. 206–221, 1990. https://doi.org/10.1115/1.2919858

[40] Chang, W. Y., Lai, J. S., Yen, C. L. "Evolution of scour depth at circular bridge piers", Journal of Hydraulic Engineering, 130(9), pp. 905–913, 2004. https://doi.org/10.1061/(ASCE)0733-9429(2004)130:9(905)

[41] Subramanya, K. "Flow in Open Channels", 3rd ed, McGraw-Hill, New York, NY, USA, 2009.

[42] Palermo, M., Pagliara, S., Bombardelli, F. A. "Theoretical approach for shear-stress estimation at 2D equilibrium scour holes in granular material due to subvertical plunging jets", Journal of Hydraulic Engineering, 146(4), pp. 1–12, 2020. https://doi.org/10.1061/(ASCE)HY.1943-7900.0001703

[43] Melville, B. W., Chiew, Y. M. "Time scale for local scour at bridge piers", Journal of Hydraulic Engineering, 125(1), pp. 59–65, 1999. https://doi.org/10.1061/(ASCE)0733-9429(1999)125:1(59)

[44] Mia, A. F., Nago, H. "Design method of time- dependent local scour at circular bridge pier", Journal of Hydraulic Engineering, 129(6), pp. 420–427, 2003. https://doi.org/10.1061/(ASCE)0733-9429(2003)129:6(420)